



HAL
open science

Role of NO₃ radical in oxidation processes in the eastern Mediterranean troposphere during the MINOS campaign

M. Vrekoussis, M. Kanakidou, N. Mihalopoulos, P. J. Crutzen, J. Lelieveld, D. Perner, H. Berresheim, E. Baboukas

► **To cite this version:**

M. Vrekoussis, M. Kanakidou, N. Mihalopoulos, P. J. Crutzen, J. Lelieveld, et al.. Role of NO₃ radical in oxidation processes in the eastern Mediterranean troposphere during the MINOS campaign. Atmospheric Chemistry and Physics Discussions, 2003, 3 (3), pp.3135-3169. hal-00301104

HAL Id: hal-00301104

<https://hal.science/hal-00301104>

Submitted on 18 Jun 2008

HAL is a multi-disciplinary open access archive for the deposit and dissemination of scientific research documents, whether they are published or not. The documents may come from teaching and research institutions in France or abroad, or from public or private research centers.

L'archive ouverte pluridisciplinaire **HAL**, est destinée au dépôt et à la diffusion de documents scientifiques de niveau recherche, publiés ou non, émanant des établissements d'enseignement et de recherche français ou étrangers, des laboratoires publics ou privés.

**Role of NO₃ radicals
in oxidation
processes**

M. Vrekoussis et al.

Role of NO₃ radical in oxidation processes in the eastern Mediterranean troposphere during the MINOS campaign

M. Vrekoussis¹, M. Kanakidou¹, N. Mihalopoulos¹, P. J. Crutzen², J. Lelieveld², D. Perner², H. Berresheim³, and E. Baboukas²

¹Environmental Chemical Processes Laboratory, Department of Chemistry, University of Crete, P.O. Box 1470, 71409 Heraklion, Greece

²Max-Planck-Institut für Chemie, Abt. Luftchemie, Mainz, Germany

³Deutscher Wetterdienst, Meteorologisches Observatorium, DWD, Germany

Received: 26 March 2003 – Accepted: 21 May 2003 – Published: 19 June 2003

Correspondence to: M. Kanakidou (mariak@chemistry.uoc.gr)

Title Page

Abstract

Introduction

Conclusions

References

Tables

Figures

◀

▶

◀

▶

Back

Close

Full Screen / Esc

Print Version

Interactive Discussion

© EGU 2003

Abstract

During the MINOS campaign (28 July–18 August 2001) nitrate (NO_3) radical was measured at Finokalia, on the north coast of Crete in South-East Europe using a long path (10.4 km) Differential Optical Absorption Spectroscopy instrument (DOAS). Hydroxyl (OH) radical was also measured by a Chemical Ionization Mass-Spectrometer (Berresheim et al., this issue). These datasets represent the first simultaneous measurements of OH and NO_3 radicals in the area. NO_3 radical concentrations ranged from less than $3 \cdot 10^7$ up to $9 \cdot 10^8$ radical $\cdot\text{cm}^{-3}$ with an average value of $1.1 \cdot 10^8$ radical $\cdot\text{cm}^{-3}$.

The observed NO_3 mixing ratios are analyzed on the basis of the corresponding meteorological data and the volatile organic compound (VOC) observations simultaneously obtained at Finokalia station. The importance of the NO_3 radical relatively to that of OH in the dimethylsulfide (DMS) and nitrate cycles is also investigated. The observed NO_3 levels clearly regulate the diurnal variation of DMS. NO_3 and N_2O_5 reactions account for about 21% of the total nitrate ($\text{HNO}_{3(\text{g})} + \text{NO}_{3(\text{part})}^-$) production.

1. Introduction

Quality of the air and climate depend on the emissions, chemical transformation and deposition of trace constituents in the atmosphere. The self-cleaning efficiency of the troposphere is important to conserve air quality both during day and night. The most important oxidant species are OH radical, NO_3 radical and ozone.

During the day, OH plays a decisive role in the cleaning mechanism of the atmosphere. On the other hand, during night its concentration is negligible. During night, NO_3 radical and O_3 are the main oxidants (e.g. Platt et al., 1984; Wayne et al., 1991; Poisson et al., 2001). NO_3 reacts with a number of VOCs initiating their night time degradation (Atkinson et al., 2000). It also contributes to the removal of NO_x (Allan et al., 1999) mainly via HNO_3 and particulate nitrate formation.

Regardless their importance, measurements of OH and NO_3 are scarce as they

Role of NO_3 radicals in oxidation processes

M. Vrekoussis et al.

Title Page

Abstract

Introduction

Conclusions

References

Tables

Figures

◀

▶

◀

▶

Back

Close

Full Screen / Esc

Print Version

Interactive Discussion

Role of NO₃ radicals in oxidation processes

M. Vrekoussis et al.

Title Page

Abstract

Introduction

Conclusions

References

Tables

Figures

◀

▶

◀

▶

Back

Close

Full Screen / Esc

Print Version

Interactive Discussion

© EGU 2003

have been proven difficult due to the very low concentrations and the high spatial and temporal variability of these radicals. Consequently the relative contribution of these two radicals to the oxidation efficiency of the atmosphere requires further investigation.

The major source of NO₃ is the oxidation of nitrogen dioxide (NO₂) by ozone (O₃):



The production rate of NO₃ (P_{NO_3}) by this reaction is given by $P_{\text{NO}_3} = k_{\text{NO}_2\text{O}_3} \cdot [\text{NO}_2] \cdot [\text{O}_3]$ and equals 0.072 ppbv NO₃ per hour, for 0.5 ppbv of NO₂ and 50 ppbv of O₃ at 298 K, conditions typical of the Mediterranean area during summertime.

10 During day, NO₃ has a very short lifetime (about 5 s) due to its strong absorption in the visible region of the solar spectrum (maximum absorption 662 nm) and rapid photodissociation, mainly to NO₂ (reaction 2a) and to a lesser extend to NO (reaction 2b):



15 In mid-latitudes near the surface the combined photolysis rate of the reactions is about $J_4 = 0.2 \text{ s}^{-1} = 720 \text{ h}^{-1}$ at noon during summer. Assuming dynamic equilibrium of NO₃ (production by reaction (1) equals loss by photo-dissociation (2a and 2b)), the daytime concentration of NO₃ is calculated to be 0.1 pptv ($P_{\text{NO}_3}/J_4 = [72 \text{ pptv h}^{-1}]/[720 \text{ h}^{-1}]$). Such low NO₃ concentration cannot be detected by the DOAS instrument as will be discussed later.

NO₃ reacts with NO₂ to produce N₂O₅ via the temperature-dependant equilibrium (Wangeberg et al., 1997):



25 Subsequent removal of nitrogen pentoxide (N₂O₅) leads to a net loss of NO₃ from the atmosphere. In the gas phase N₂O₅ can contribute to nitric acid formation following

first and second order reactions with water vapour (Wahner et al., 1998):



Additional HNO_3 formation paths involve VOC reactions with NO_3 and particularly DMS, aldehydes and higher alkanes (H – abstraction mechanism) as well as heterogeneous reactions of NO_3 or N_2O_5 on particles (Heintz et al., 1996). The NO_3 reaction with unsaturated VOC proceeds via addition of NO_3 to the double C bound and does not produce HNO_3 .

Several authors reported important interactions between nitrogen and sulfur cycles in the marine atmosphere via the NO_3 radical (Yvon et al., 1996; Carslaw et al., 1997; Allan et al., 1999, 2000). For instance, Allan et al. (1999) calculated that at NO_x levels exceeding 100 pptv, conditions typical of the marine atmosphere in the Northern Hemisphere, OH and NO_3 radicals are expected to equally contribute to the loss of DMS. The NO_3 radical contributes also to HNO_3 production during night as was shown by Allan et al. (2000).

As part of the MINOS experiment daily measurements of ambient NO_3 concentrations were conducted during summer 2001, at the ground level station at Finokalia on the northeastern coast of Crete. The aim was to study the NO_3 occurrence in the Mediterranean marine boundary layer, to evaluate the NO_3 role in the oxidation efficiency of the atmosphere and provide insights in the interactions between S and N cycles. To achieve these goals simultaneous measurements of OH, DMS, NO_2 , gaseous HNO_3 and particulate NO_3 have been performed during a one-month period.

**Role of NO_3 radicals
in oxidation
processes**

M. Vrekoussis et al.

Title Page

Abstract

Introduction

Conclusions

References

Tables

Figures

⏪

⏩

◀

▶

Back

Close

Full Screen / Esc

Print Version

Interactive Discussion

2. Experimental

2.1. Setup of the long path DOAS instrument

The NO₃ radical mixing ratio has been monitored continuously by using a long path DOAS instrument at Finokalia (35.3' N, 25.3' E), Crete, Greece, 150 m above sea level, from 28 July to 18 August 2001 (Fig. 1). The monitoring station of the University of Crete at Finokalia is located 70 km eastward of Heraklion and 25 km west of Agios Nikolaos, the nearest big cities in the area.

The DOAS instrument used during MINOS was provided by MPI Mainz and has been used in the past in several campaigns. The details of its operation have been presented elsewhere (Martinez et al., 2000); here only a short description is given. The DOAS uses a parabolic mirror behind a Xenon high pressure lamp (supplied by Hanovia, 500W) to produce a parallel light beam (Fig. 2). At a distance of 5.2 km, an array of 30 retro-reflectors of 5 cm diameter reflects the main beam backwards at the sending point (total light path is 10.4 km) where another parabolic mirror focuses the light to the optical fibre in front of the collecting mirror. Through an optical fibre (inner diameter 600 μm) the light is transmitted to the spectrograph and then to the detector. The spectrograph is based on a holographic lattice of the Fa. American Holographic (455.01, 240–800 nm) with a focal length of 212 mm, a linear dispersion of 7 nm mm⁻¹ and a diffraction grating with 550 grooves mm⁻¹. The detector used to record the data is a 1024 pixel photodiode array (PDA, RY-1024, Hamamatsu), fixed to the focal plane of the spectrograph and cooled to -20° C to minimize the dark current.

The spectrum (N) used for the calculation of the species of interest has been obtained using the following equation $N = \frac{M-S}{L-O}$ where:

- *M* is the atmospheric spectrum measured when the light path is focused on the centre of the fibre and contains scattered light.
- *S* is the scattered light measured when the light path is shifted mechanically from the centre of the fibre by focusing more than about 1 cm far from it.

Role of NO₃ radicals in oxidation processes

M. Vrekoussis et al.

Title Page

Abstract

Introduction

Conclusions

References

Tables

Figures

◀

▶

◀

▶

Back

Close

Full Screen / Esc

Print Version

Interactive Discussion

- O is the offset measured when the fibre is lidded by a black cover.
- L is the Lamp spectrum measured when the fibre is mounted directly to the lamp.

The N spectrum is then smoothed by fast Fourier transform, firstly with a high pass frequency filter and secondly, with a low pass frequency filter in order to remove i) high-frequency noise from the variability of the diode arrays, ii) adjacent border spectral trends caused by Rayleigh and Mie scattering in the atmosphere and iii) detector etaloning. Every measurement is the mean value of nineteen individual ones and, on average, lasted 30 min.

The method used to obtain the final spectrum containing the information for the species of interest is the multi-scanning technique described in detail by Martinez-Harder (1998) and Brauers et al. (1995).

NO_3 radical is detected in the visible spectral range. Two absorption peaks have been identified in the red region at 662 and 623 nm. In this work the NO_3 absorption band ($B_2E' - X^2A'_2$) at 662 nm is used for the NO_3 evaluation. Apart from NO_3 radical, the main absorbers in that region (620-670) nm are water vapour and NO_2 , and these species are fitted along with NO_3 in the analysis routine. The influence of water is much more critical for NO_3 than that of NO_2 because overtone vibrational bands of water peak at 651.5 nm, very close to NO_3 . Since the concentration of NO_3 during daytime is negligible due to its rapid photolysis, daytime reference spectra (collected several times per day) are used as references for the humidity in the deconvolution procedure. These reference spectra are then fitted and subtracted from the night time spectra to derive the spectrum containing only NO_3 radical data. The thus derived optical density of this peak and the NO_3 cross sections reported by Yokelson et al. (1994) are used to determine NO_3 radical concentration. In practice the reference spectra for H_2O and NO_3 are fitted simultaneously using a least-squares fitting routine that employs singular value decomposition. The instrumental noise (σ) that determines the detection limit of the method is deduced from the residual background spectrum. This is calculated by further subtracting the NO_3 radical spectrum and corresponds to 0.4 pptv, which leads

Role of NO_3 radicals in oxidation processes

M. Vrekoussis et al.

[Title Page](#)[Abstract](#)[Introduction](#)[Conclusions](#)[References](#)[Tables](#)[Figures](#)[◀](#)[▶](#)[◀](#)[▶](#)[Back](#)[Close](#)[Full Screen / Esc](#)[Print Version](#)[Interactive Discussion](#)

to a detection limit (3σ) of 1.2 pptv.

Nitrogen dioxide was measured also using the DOAS technique. The procedure is similar as above except that NO_2 has also clear peaks in the UV region. NO_2 was calculated from its peak at 405 nm with a cross section of $6.38 \cdot 10^{-19} \text{ cm}^2$ (Yoshino et al., 1997). The mean instrumental noise (σ) in the case of NO_2 has been estimated to be 80 pptv, which leads to a detection limit (3σ) of 240 pptv.

2.2. Ancillary measurements

DMS was collected into 6-liter stainless steel electropolished canisters and analysed following the procedure described in details by Kouvarakis and Mihalopoulos (2000) and Bardouki et al. (this issue). Every hour one sample was analysed and the detection limit was 1 pptv. Gaseous HNO_3 was analysed using the nebulization/reflux (Cofer mist) technique described in Cofer et al. (1985) and Sciare and Mihalopoulos (1999). A $0.5 \mu\text{m}$ PTFE filter was mounted in front of the Cofer line to collect aerosols. Gaseous HNO_3 was trapped by the mist and was analyzed as nitrate by Ion Chromatography. Simultaneously the PTFE filter situated in front of the Cofer sampler was extracted with MQ-water and analysed for nitrate using Ion Chromatography. Details on the analytical procedure can be found in Kouvarakis et al. (2000).

The meteorological data was obtained by an automatic meteorological station, which recorded ambient air temperature (T), relative humidity (RH), wind speed, wind direction and the direct solar radiation. Description of the available data during the MINOS, useful for the NO_3 analysis, the used analytical techniques and the corresponding detection limits are presented in Table 1.

Role of NO_3 radicals in oxidation processes

M. Vrekoussis et al.

Title Page

Abstract

Introduction

Conclusions

References

Tables

Figures

◀

▶

◀

▶

Back

Close

Full Screen / Esc

Print Version

Interactive Discussion

3. Results

3.1. Measurements

NO₃ radical measurements were performed from 28 July to 17 August 2001 (Fig. 3). The detection limit (3 times the noise) is also shown in Fig. 3. A large daily as well as hourly variability of NO₃ has been observed, ranging from values below the detection limit (1.2 pptv) up to 37 pptv. The maximum value has been observed during the night of 11 to 12 August 2001. This event will be discussed in detail below. Table 2 compiles the NO₃ radical measurements reported for various locations around the world and compares them with our measurements. Our NO₃ observations appear to be within the range of the reported data for the planetary boundary layer.

3.2. Diurnal variation of NO₃

Daytime NO₃ levels were below the detection limit throughout the campaign (Fig. 4). NO₃ increased during sunset and reached up to several tens of pptv during night. It decreased rapidly again during sunrise due to photodissociation. Similar diurnal tendencies have been reported by several authors in coastal areas (Heinz et al., 1998; Allan et al., 1999, 2000). For comparison, Fig. 4 presents the mean diurnal variation of OH radicals (blue line) during the campaign. A detailed presentation of the OH measurements can be found in Berresheim et al. (this issue). OH levels showed a strong diurnal variability with maxima (approximately 2×10^7 molecules cm⁻³) occurring around 13:30 local time and nighttime values below the detection limit. During the entire OH measurement period (6–21 August), the mean and standard deviation were $4.5 \pm 1.1 \times 10^6$ molecules cm⁻³, i.e. a factor of 12 lower than the NO₃ levels. Most of the reactions of NO₃ with VOCs have rate constants that are between 5 and 1000 times slower than the corresponding reactions with OH (Atkinson et al., 2003 – IUPAC recommendations). Thus according to the NO₃ and OH levels observed during this study the destruction rates of some VOCs are more important during night than during

Title Page

Abstract

Introduction

Conclusions

References

Tables

Figures

⏪

⏩

◀

▶

Back

Close

Full Screen / Esc

Print Version

Interactive Discussion

day.

A very useful diagnostic for analyzing field observations of NO_3 is to calculate the atmospheric lifetime of the radical. As suggested by Platt et al. (1980), when NO_3 chemistry is in steady state, its lifetime $\tau(\text{NO}_3)$ is given by:

$$\tau(\text{NO}_3) = [\text{NO}_3]_{\text{ss}} / (K_1[\text{NO}_2][\text{O}_3]).$$

The mean values (with one standard deviation) of NO_3 and NO_2 observed during the campaign and used to calculate the lifetime $\tau(\text{NO}_3)$ are depicted in Figs. 5a, b. The calculated $\tau(\text{NO}_3)$ during the MINOS campaign is found to range between 1 and 5 min; Fig. 5c. This very short lifetime of NO_3 actually supports the steady state assumption and is reproduced by the modelling study presented below. The calculated $\tau(\text{NO}_3)$ is in good agreement with the average of 4.2 min reported by Heintz et al. (1996) from long-term observations of NO_3 at the island of Rügen in the Baltic Sea. The balance between production and loss of NO_3 can also be investigated by correlating NO_3 levels with the production rate $P_{(\text{NO}_3)}$. No significant correlation was observed during the MINOS campaign indicating a key role of removal processes in regulating NO_3 levels (Martinez et al., 2000; Heintz et al., 1996).

3.3. Meteorological parameters and impacts on NO_3

Temperature, relative humidity (RH), wind direction and speed and solar radiation were continuously monitored at Finokalia during MINOS campaign. Temperature ranged between 22.5°C and 31.5°C (mean = 25.7°C), whereas RH varied from 20 to 90% (mean = 62%). The temperature changes observed during MINOS (9°C between the maximum and minimum temperature) are not expected to critically affect NO_3 variability. However, if we consider the rates of NO_3 conversion to N_2O_5 (reaction 3) and of N_2O_5 thermal decomposition (reaction -3), we can calculate the NO_2 levels needed to reach equilibrium ($K_{3\text{eq}}$). These levels are given in Table 3 and are significantly higher than the geometric mean value of 0.4 ppbv of NO_2 observed during MINOS. The corresponding lifetimes of NO_3 and N_2O_5 for the reactions (3) and (-3) and the observed

**Role of NO_3 radicals
in oxidation
processes**

M. Vrekoussis et al.

Title Page

Abstract

Introduction

Conclusions

References

Tables

Figures

◀

▶

◀

▶

Back

Close

Full Screen / Esc

Print Version

Interactive Discussion

**Role of NO₃ radicals
in oxidation
processes**

M. Vrekoussis et al.

Title Page

Abstract

Introduction

Conclusions

References

Tables

Figures

◀

▶

◀

▶

Back

Close

Full Screen / Esc

Print Version

Interactive Discussion

© EGU 2003

mean value of NO₂ are also reported in Table 3. Interestingly during the whole MI-NOS experiment, the characteristic time for the NO₃ conversion to N₂O₅ is 3 to 9 times slower than the thermal decomposition of N₂O₅ to NO₃. Thus, the equilibrium favours NO₃ rather than N₂O₅ as would have been expected at lower temperatures and/or higher NO₂ levels and had been the case for most campaigns that reported NO₃ measurements as presented in Table 2. The high NO₃ concentrations observed near 12 August 2001 point to elevated temperature as the main cause due to thermal dissociation of N₂O₅. In Fig. 6a we depicted the correlation between NO₃ concentrations integrated every 10°C of temperature. In addition to temperature, RH varied by almost a factor of 4.5. Figure 6b presents both the variation of NO₃ radical and that of RH. It is interesting to note that the maximum NO₃ mixing ratio of 37 pptv has been observed on 11–12 August 2001 when RH was the lowest observed during the experiment. To further illustrate the role of humidity on NO₃, Fig. 6c presents the correlation between NO₃ and RH, with NO₃ values integrated every 10 units of RH. A highly significant linear relationship is then observed with NO₃ decreasing by almost a factor of 3 when RH increases from 20-30% to 80-90% indicating the importance of both gas phase reactions of N₂O₅ with H₂O and reactions of N₂O₅ on particles since the hygroscopic growth of aerosols increases the surface available for heterogeneous reactions. To further understand this negative correlation we reported in Table 4 the pseudo first order rate of N₂O₅ gas phase reaction with H₂O together with the corresponding lifetime of N₂O₅. The lifetime of N₂O₅ with respect to the gas phase reaction with water into HNO₃ is reduced by a factor of 3 (from 1235 to 424 s) when temperature and relative humidity vary from their minimum to their maximum values as observed during MINOS, which could explain the observed negative correlation of NO₃ with humidity depicted in Fig. 6c.

3.4. Impact of DMS and others VOC on NO₃ oxidation

DMS is the dominant sulfur gas naturally emitted into the atmosphere. It is formed by biological processes in the sea water from dimethylsulfoniopronate (DMSP). The

potential role of DMS in the CCN production but also in the acidity of rainwater in remote marine areas has been intensively studied since the publication of the CLAW hypothesis involving the influence of DMS oxidation products on climate (Charlson et al., 1987).

5 Platt and Le Bras (1997) suggested a potentially important role of DMS in the $O_x - NO_y$ partitioning in the marine background atmosphere. Cantell et al. (1997) pointed out the contribution of NO_3 initiated oxidation of DMS to nighttime RO_2 formation. Allan et al. (1999, 2000) found that DMS levels can significantly affect the NO_3 lifetime. Especially under condition of elevated DMS (> 100 pptv), a major fraction of
10 NO_3 (up to 90%) is removed by reaction with DMS. During MINOS 2001, measurements of DMS were conducted in parallel with the NO_3 radical observations. Figure 7 depicts the mean diurnal variation of DMS and NO_3 during MINOS campaign. During sunset DMS decreases from more than 30 pptv down to about 5 pptv when NO_3 radicals build up, reflecting significant DMS night time oxidation by NO_3 leading to HNO_3 and possibly lower DMS fluxes during night due to dilution by continental air. Such a diurnal variation was observed during the entire campaign, and more details are reported in a companion paper (Bardouki et al., this issue). By considering the observed mean DMS concentration of 30 pptv during the campaign a lifetime of about 10^3 s is estimated for NO_3 radicals, which is longer by almost a factor of 5–10 than that calculated
20 during the campaign and depicted in Fig. 5c. NO_3 radicals can also be removed by a variety of VOCs especially by isoprene and terpenes. During the campaign isoprene levels were very low (about 7 pptv; Gros et al., this issue). No terpenes were measured during the campaign but their levels are expected to be very low since the surrounding vegetation is sparse and consists mainly of some dry herbs and low bushes. These
25 results indicate that gas-phase reactions of DMS and most probably other VOCs with NO_3 radicals play a relatively minor role in the NO_3 budget and that most NO_3 is removed from the atmosphere via reactions of N_2O_5 with water vapour and/or NO_3 and N_2O_5 on aerosol surfaces.

**Role of NO_3 radicals
in oxidation
processes**M. Vrekoussis et al.

[Title Page](#)[Abstract](#)[Introduction](#)[Conclusions](#)[References](#)[Tables](#)[Figures](#)[◀](#)[▶](#)[◀](#)[▶](#)[Back](#)[Close](#)[Full Screen / Esc](#)[Print Version](#)[Interactive Discussion](#)

3.5. Impact of NO₃ on HNO₃ formation

To investigate the NO₃ budget and to evaluate the NO₃ involvement in HNO₃ formation, box model simulations have been performed.

3.5.1. The model

5 The chemical scheme used for this purpose is based on Poisson et al. (2001) as updated by Tsigaridis and Kanakidou (2001) for the inorganic and hydrocarbon chemistry (up to C₅) including NO₃ radical reactions with peroxy radicals. Reaction rates have been updated according to Atkinson et al. (2003) (IUPAC, web version 2003) recommendations. Table 5 presents the gas phase reactions of NO₃ considered in the
10 model. The N₂O₅ gas phase reactions with H₂O (1st and 2nd order with respect to H₂O, Eqs. 6a and 6b) considered by using a pseudo first order reaction as suggested by Heinz et al. (1996) as well as the heterogeneous reactions of NO₃, N₂O₅ and HNO₃ listed in Table 6 are also taken into account. Deposition of HNO₃, NO₃, N₂O₅ and NO₃⁻ (particulate) onto surfaces has been considered with deposition velocities of 1 cm s⁻¹
15 for the gases and 3 times higher for the particles since most NO_{3(part)}⁻ is on coarse sea-salt particles (Bardouki et al., 2003b).

Observed hourly mean values of O₃, photolysis rates of NO₂ (JNO₂) and O₃ (JO¹D) and CO are used as input to the model that is also forced every 5-min by the geometric hourly mean value of NO₂ measured by the DOAS instrument. Missing NO₂
20 data have been substituted by extrapolating the observations on the basis of the diurnal mean normalized profile of NO₂ measured during the campaign. Isoprene, ethene, propene, formaldehyde, acetaldehyde, ethane, propane and butane mixing ratios are kept equal to 7, 100, 50, 1000, 100, 1000, 260 and 120 pptv, respectively, according to observations during the MINOS campaign (Gros et al., this issue) and in the
25 West Mediterranean (Plass-Dümler et al., 1992). Aerosol surfaces observed during the campaign (Bardouki et al., this issue) are used to calculate the heterogeneous re-

Title Page

Abstract

Introduction

Conclusions

References

Tables

Figures

◀

▶

◀

▶

Back

Close

Full Screen / Esc

Print Version

Interactive Discussion

**Role of NO₃ radicals
in oxidation
processes**M. Vrekoussis et al.

[Title Page](#)[Abstract](#)[Introduction](#)[Conclusions](#)[References](#)[Tables](#)[Figures](#)[◀](#)[▶](#)[◀](#)[▶](#)[Back](#)[Close](#)[Full Screen / Esc](#)[Print Version](#)[Interactive Discussion](#)

© EGU 2003

removal rates for the reactions listed in Table 6. Diurnal mean DMS observations were used to account for the DMS emitted by the ocean and its impact on NO₃ chemistry in the marine boundary layer. DMS oxidation both by OH radical and by NO₃ radical is taken into account (see reaction rates in Table 5). Initial concentrations of hydrogen peroxide (495 pptv), methane (1.8 ppmv) and particulate nitrate (25 nmol m⁻³) are applied.

3.5.2. Model results

The model satisfactorily simulates the daytime variation and the absolute concentrations of OH radicals as shown in Fig. 8, although overall it underestimates the observations of OH radical by about 8%. Details of OH radical measurements are reported by Berresheim et al. (this issue).

3.5.2.1. NO₃ model versus observations

NO₃ radical concentrations simulated by the model for the whole period are shown in Fig. 9 together with the observed NO₃ values (all 15 min data). When neglecting the NO₃ values observed during the nights of 11 and 12 of August 2001 that are exceptionally high for the period, an overall good agreement between model results and observations is apparent. The mean NO₃ concentration of 4.5 pptv (all data) observed during night is in quite good agreement with the 4.7 pptv simulated by the model for the same period. When comparing the hourly mean observed concentrations to the hourly model output a linear regression with a slope of 0.98 is deduced, although the scatter of data is important ($r^2 = 0.4$, $n=161$).

3.5.2.2. Losses of NO₃

According to our calculations photolysis of NO₃ is by far the major loss mechanism during daytime since it accounts for more than half the total removal of NO₃

**Role of NO₃ radicals
in oxidation
processes**

M. Vrekoussis et al.

and N₂O₅. During night the relative importance of the various paths of NO₃ and N₂O₅ loss is changing but generally N₂O₅ heterogeneous and gas phase losses (to molecules other than NO₃) are almost a factor of 2 higher than the reaction of NO₃ with DMS. This relatively small contribution of DMS to NO₃ loss (less than 25%) compared to earlier published estimates by Carslaw et al. (1997) reflects the different conditions encountered during the studies with regard to the DMS levels (the lowest have been observed during MINOS) and the length of the night over which this reaction is important (shortest during our study). Under the studied conditions other VOC reactions with NO₃ seem to be of minor importance in the NO₃ budget.

3.5.2.3. HNO₃ and NO₃⁻ (particulate) model versus observations

The contribution of NO₃ nighttime reactions with VOC (including DMS), leading to HNO₃ formation has also been investigated on the basis of the model results. The model simulates within 10% the observed levels of the sum of the gaseous HNO₃ and the particulate NO₃⁻ (NO_{3(part)}). The best agreement is achieved for the period 28 July to 1 August 2001. Thus, to investigate the NO₃ involvement in the HNO₃ production, we focus on this first period of the campaign when the model appears to realistically simulate the sum of gaseous HNO₃ and particulate NO₃⁻. According to our calculations HNO₃ is predominantly formed during daytime by reaction of NO₂ with OH at a rate of 1.12 ppbv/d. DMS oxidation by NO₃ radicals is an important source of HNO₃ during night, producing 0.11 ppbv/d of HNO₃ whereas 0.10 ppbv/d of HNO₃ is due to the gas phase reactions of N₂O₅ with water vapour. The NO₃ heterogeneous reaction appears to be minor since it does not produce more than 1 pptv/d of HNO₃. The overall HNO₃ production is calculated to be 1.3 ppbv/d. NO₃ and N₂O₅ gas phase reactions constitute the nighttime chemical source for HNO₃ and contribute therefore approximately 16% to the HNO₃ production (Fig. 10a). Under the studied conditions, the reactions of NO₃ with aldehydes are minor for HNO₃ production since only 3 and 1 pptv/d are produced during the NO₃ initiated oxidation of formaldehyde

[Title Page](#)[Abstract](#)[Introduction](#)[Conclusions](#)[References](#)[Tables](#)[Figures](#)[◀](#)[▶](#)[◀](#)[▶](#)[Back](#)[Close](#)[Full Screen / Esc](#)[Print Version](#)[Interactive Discussion](#)

**Role of NO₃ radicals
in oxidation
processes**

M. Vrekoussis et al.

[Title Page](#)[Abstract](#)[Introduction](#)[Conclusions](#)[References](#)[Tables](#)[Figures](#)[◀](#)[▶](#)[◀](#)[▶](#)[Back](#)[Close](#)[Full Screen / Esc](#)[Print Version](#)[Interactive Discussion](#)

© EGU 2003

and higher aldehydes, respectively. Fig. 10b depicts the mean diurnal variation of the HNO₃ production rates, which reveals the importance of the NO₃ and N₂O₅ reaction for HNO₃ formation during nighttime. The calculated HNO₃ daytime production rate of 1.12 ppbv/d during the MINOS campaign is more than double that suggested by Carslaw et al. (1997) for lower photochemical activity conditions (less OH radicals than during MINOS). However, the DMS contribution to HNO₃ formation via H- abstraction by NO₃ radicals is lower than the estimate by Carslaw et al. (1997). This difference is due to high DMS concentrations that resulted from a phytoplankton bloom in the area studied by these authors. Thus our results, although different from that earlier study, are fully consistent when taking into account the particularities of the studied environments.

The heterogeneous reaction of N₂O₅ ($\gamma = 0.1$) on particles does not produce more than 0.09 ppbv/d of particulate NO₃⁻ (NO_{3(part)}⁻). Therefore, by considering the overall HNO_{3(g)} + NO_{3(part)}⁻ production, N₂O₅ and NO₃ reactions contribute up to 21%, whereas the remaining is attributed to the NO₂ reaction with OH during daytime.

With regard to HNO₃ loss from the atmosphere, reaction with OH and photolysis are calculated to play only a minor role in the total loss of HNO₃ (2% and 1%, respectively) whereas its main removal mechanism (97%) is conversion to particulate NO₃⁻ and subsequent deposition.

4. Conclusions

During the MINOS campaign from 27 July to 17 August 2001, a complete set of NO₃ data was obtained by a DOAS instrument, indicating NO₃ levels that vary from the detection limit up to 37 pptv. The 24-hour mean NO₃ levels were a factor of 12 higher than these of the OH radical. Thus for some compounds such as DMS the nighttime destruction by NO₃ is much more important than loss by OH during daylight. The role of NO₃ to the overall oxidation efficiency of the Mediterranean atmosphere on a yearly basis is topic for further research since preliminary measurements show a much

**Role of NO₃ radicals
in oxidation
processes**

M. Vrekoussis et al.

smaller seasonal variation for NO₃ compared to OH radical.

The calculated lifetime of NO₃ during the MINOS campaign ranges between 1 and 5 min, supporting the assumption of steady state conditions between production and destruction of NO₃. Gas-phase reactions of DMS and most probably other VOCs with NO₃ radicals appear to play a minor role in the NO₃ budget, since the major fraction of NO₃ is removed from the atmosphere via N₂O₅ reactions.

NO₃ radical was found to be strongly anti-correlated with the relative humidity (RH). High values of RH are associated with efficient loss of NO₃, reducing it to levels down to the detection limit. This indicates that both gas phase reactions of N₂O₅ with H₂O and reactions of NO₃ and N₂O₅ on particles are important since the hygroscopic growth of aerosols increases the surface available for heterogeneous reactions.

N₂O₅ and NO₃ reactions contribute up to 21% to the total formation rate of HNO_{3(g)} + NO_{3(part)}⁻, while the remaining and thus major part is attributed to the NO₂ reaction with OH during daytime. The contribution of N₂O₅ and NO₃ reactions to the overall HNO_{3(g)} + NO_{3(part)}⁻ production on a seasonal basis deserves further study.

Acknowledgements. We wish to thank T. Klupfel for assistance with the DOAS instrument, H. Bardouki, V. Gros, G. Kouvarakis, K. Oikonomou and J. Sciare for communicating the DMS, HNO₃, NO_{3(part)}⁻ and VOC data prior publication, U. Platt for helpful discussions, the Research Committee of the University of Crete, and the Greek secretary of research and Technology (PENED grant) for financial support. M. Vrekoussis acknowledges support by DAAD for education visits to MPI-Mainz.

References

- Allan, B., Carslaw, N., Coe, H., Burgess, R., and Plane, J.: Observations of the Nitrate Radical in the marine boundary layer, *J. Atmos. Chem.* 33, 129–154, 1999.
- Allan, B. J., Mc Figgans, G., Plane, J., Coe, H., Mc Fadyen: The nitrate radical in the remote marine boundary layer, *J. Geophys.Res.*, 105, D19, 24 191–24 204, 16 October, 2000.

[Title Page](#)[Abstract](#)[Introduction](#)[Conclusions](#)[References](#)[Tables](#)[Figures](#)[◀](#)[▶](#)[◀](#)[▶](#)[Back](#)[Close](#)[Full Screen / Esc](#)[Print Version](#)[Interactive Discussion](#)

© EGU 2003

**Role of NO₃ radicals
in oxidation
processes**M. Vrekoussis et al.

[Title Page](#)[Abstract](#)[Introduction](#)[Conclusions](#)[References](#)[Tables](#)[Figures](#)[◀](#)[▶](#)[◀](#)[▶](#)[Back](#)[Close](#)[Full Screen / Esc](#)[Print Version](#)[Interactive Discussion](#)

© EGU 2003

- Atkinson, R.: Kinetic and mechanism of gas-phase reactions of NO₃ radical with organic compounds, *J. Physical Chem.*, 20, 459–507, 1991.
- Atkinson, R., Baulch, D. L., Cox, R. A., Crowley, J. N., Hampson, R. F., Kerr, J. A., Rossi, M. J., and Troe, J.: IUPAC recommendations, <http://www.iupac-kinetic.ch.cam.ac.uk/>, 2003.
- 5 Bardouki, H., Berresheim, H., Sciare, J., Vrekoussis, M., Kouvarakis, G., Oikonomou, C., Schneider, J., and Mihalopoulos, N.: Gaseous (DMS, DMSO, SO₂, H₂SO₄, MSA) and particulate (MS⁻ and SO₄²⁻) sulfur compounds during the MINOS campaign, *ACP*, this issue.
- Bardouki, H., Liakakou, H., Economou, C., Sciare, J., Smolik, J., Zdimal, V., Eleftheriadis, K., Lazaridis, M., Dye, C., and Mihalopoulos, N.: Chemical composition of size-resolved atmospheric aerosols in the eastern Mediterranean during summer and winter, *Atmos. Environ.*, 10 37, 195–208, 2003b.
- Berresheim, H., Elste, T., Plass-Dülmer, C., Eisele, F. L., and Tanner, D. J.: Chemical ionization mass spectrometer for long-term measurements of atmospheric OH and H₂SO₄, *Int. J. Mass Spectrom.*, 202, 91–103, 2000.
- 15 Berresheim, H., Plass-Dülmer, C., Elste, T., Mihalopoulos, N., and Rohrer, F.: OH in the coastal boundary layer of Crete during MINOS: Measurements and relationship with ozone photolysis, *ACP*, this issue.
- Brauers, T., Hausmann, M., Brandenburger, U., and Dorn, H.-P.: Improvement of Differential Optical Spectroscopy with a multichannel scanning technique, *Appl. Opt.*, 34, 4472–4479, 20 1995.
- Cantrell, C. A., Shetter, R. E., Calvert, J. G., Eisele, F. L., and Tanner, D. J.: Some considerations of the origin of nighttime peroxy radicals observed in MILOPEX 2c, *J. Geophys. Res.*, 102, 15 899–15 913, 1996.
- Carlsaw, N., Plane, J., Coe, H., and Cuevas, E.: Observation of the nitrate radical in the free troposphere, *J. Geophys. Res.*, 102, D9, 10 613–10 622, 1997.
- 25 Charlson, R. J., Lovelock, J. E., Andreae, M. O., and Warren, S. G.: Oceanic phytoplankton, atmospheric sulphur, cloud albedo and climate: a geophysiological feedback, *Nature*, 326, 655–661, 1987.
- Cofer III, W. R., Collins, V. G., and Talbot, R. W.: An improved aqueous scrubber for the collection of soluble atmospheric trace gases, *Environ. Science Technology*, 19, 557–560, 1985.
- 30 DeMore, W. B., Sander, S. P., Golden, D. M., Hampson, R. F., Kyrylo, M. J., Howard, C. J., Ravishankara, A. R., Kolb, C. E., and Molina, M. J.: Chemical kinetics and photochemical data for use in stratospheric modeling, *Eval.* 11, *Jet Propul. Lab.*, Pasadena, Calif., 1997.

**Role of NO₃ radicals
in oxidation
processes**M. Vrekoussis et al.

[Title Page](#)[Abstract](#)[Introduction](#)[Conclusions](#)[References](#)[Tables](#)[Figures](#)[◀](#)[▶](#)[◀](#)[▶](#)[Back](#)[Close](#)[Full Screen / Esc](#)[Print Version](#)[Interactive Discussion](#)

© EGU 2003

Geyer, A., Ackermann, R., Dubois, R., Lohrmann, B., Muller, T., and Platt, U.: Long term observation of Nitrate radicals in the continental layer near Berlin, *Atmos. Environ.*, 35, 3619–3631, 2001.

Gros, V., Williams, J., Krol, M., Berresheim, H., Salisbury, G., Hofmann, R., and Lelieveld, J.: Investigating source origins and photochemical processing of the VOCs during the MINOS, ACP, this issue.

Heintz, F., Platt, U., Flentje, H., and Dubois, R.: Long term observation of Nitrate radicals at the Tor Stations, Kap Arkona (Rügen), *J. Geophys. Res.*, 101, D17, 22 891–22 910, 1996.

Kouvarakis, G. and Mihalopoulos, N.: Seasonal variation of dimethylsulfide in the gas phase and of methanesulfonate and non-sea-salt sulfate in the aerosol phase measured in the eastern Mediterranean atmosphere, *Atmos. Environ.*, 36, 929–938, 2002.

Martinez, M., Perner, D., Hackenthal, E., Kutzer., S., and Schultz, L.: NO₃ at Helgoland during the NORDEX campaign in October 1996, *J. Geophys. Res.*, 105, D18, 22 685–22 695, 2000.

Martinez-Harder, M.: Ph.D thesis, Messungen von BrO und anderen Spurenstoffen in der bodennahen Troposphäre, Max Planck-Institute for Chemistry, Mainz, 1998.

Platt, U. and Le Bras, G.: Influence of DMS on the O_x – NO_y partitioning and the NO_x distribution in the marine background atmosphere., *Geophys. Res. Letters*, 24, 1935–1938, 1997.

Platt, U., Winer, A. M., Biermann, H. W., Atkinson, R., and Pitts, J.: Measurements of nitrate radical concentrations in continental air, *Environ. Science Technology*, 18, 365–369, 1984.

Platt, U., Perner., D., Harris., G. W., Winer, A. M., and Pitts, J. M.: Detection of NO₃ in the polluted troposphere by differential optical absorption, *Geophys. Res. Letters*, 7, 89–92, 1980.

Plass-Dümler, C., Ratte, M., Koppmann, R., and Rudolph, J.: C₂ – C₉ Hydrocarbons in the Marine atmosphere during NATAC 91, paper presented at the NATAC 91 workshop, Odessa, Ukraine, 1992.

Poisson, N., Kanakidou, M., Bonsang, B., Behmann, T., Burrows, J. P., Fischer, H.; Golz, C., Harder, H., Lewis, A., Moortgat, G. K., Nunes, T., Pio, C. A., Platt, U., Sauer, F., Schuster, G., Seakins, P., Senzig, J., Seuwen, R., Trapp, D., Volz-Thomas, A., Zenker, T., and Zitzelberger, R.: The impact of natural non-methane hydrocarbon oxidation on the free radical and ozone budgets above a eucalyptus forest, *Chemosphere: Global Change Science*, Elsevier Science, 3, 353–366, 2001.

Sciare, J. and Mihalopoulos, N.: Atmospheric Dimethylsulfoxide (DMSO): An improved method for Sampling and analysis, *Atmos. Environ.*, 34, 151–156, 2000.

- Tsigaridis, K. and Kanakidou, M.: Importance of Volatile Organic Compounds Photochemistry Over a Forested Area in Central Greece, *Atmos. Environ.*, 36, 19, 3137–3146, 2002.
- Wahner, A., Mentel, T. F., and Sohn, M.: Gas-phase reaction of N_2O_5 with water vapour: importance of heterogeneous hydrolysis of N_2O_5 and surface deposition of HNO_3 in a large Teflon chamber, *Geophys. Res. Letters*, 25, 2169–2172, 1998a.
- Wangeberg, I., Etzkorn, T., Barnes, I., Platt, U., and Becker, K.: Absolute determination of the temperature behavior of the $\text{NO}_2 + \text{NO}_3^- + (\text{M}) \rightarrow \text{N}_2\text{O}_5 + (\text{M})$ equilibrium., *J. Phys. Chem. A*, 101, 9694–9698, 1997.
- Wayne, R. P., Barnes, I., Biggs, P., Burrows, J. P., Canasa-Mas, C. E., Hjorth, J., Le Bras, G., Moorgat, G. K., Perner, D., Poulet, G., Restelli, G., and Sidebottom, H.: The nitrate radical physics, chemistry, and the atmosphere, *Atmos. Environ.*, 25A, 1–203, 1991.
- Yokelson, R. J., Burkholder, J. B., Fox, R. W., Talukdar, R. K., and Ravisankara, A. R.: Temperature dependence of the NO_3 radical, *J. Phys. Chem.*, 98, 13 144–13 150, 1994.
- Yoshino, K., Esmond, J. R., and Parkinson, W. H.: High resolution absorption cross section measurements of NO_2 in the UV and VIS region, *Chemical Physics*, 221, 169–174, 1997.
- Yvon, S. A., Plane, J. M. C., Nien, C.-F., Cooper, D. J., and Saltzman, E. S.: Interaction between nitrogen and sulphur cycles in the polluted marine boundary layer, *J. Geophys. Res.*, 101, 3, 1379–1386, 1996.

**Role of NO_3 radicals
in oxidation
processes**M. Vrekoussis et al.

[Title Page](#)[Abstract](#)[Introduction](#)[Conclusions](#)[References](#)[Tables](#)[Figures](#)[◀](#)[▶](#)[◀](#)[▶](#)[Back](#)[Close](#)[Full Screen / Esc](#)[Print Version](#)[Interactive Discussion](#)

Role of NO₃ radicals in oxidation processes

M. Vrekoussis et al.

Table 1. Measurements during MINOS relevant to the present analysis

Measurement	Technique	Detection limit time resolution used
NO,NO _y	Chemiluminescent detector	50 pptv-5 min
NO ₂	DOAS	250 pptv-15 min
NO ₃	DOAS	1.5 pptv-30 min
O ₃	UV photometer	1 ppbv-5 min
DMS	GC-FPD	1 pptv-60 min
OH	Chemical Ionization Mass Spectrometry (SI/CIMS)	$2.4 \cdot 10^5$ rad/cm ³ (2 σ)-5 min
T, R.H, wind speed, wind direction, solar irradiance	Meteorological station	5 min
J(NO ₂), J(O ¹ D)	2 π radiometer	5 min

Title Page

Abstract

Introduction

Conclusions

References

Tables

Figures

◀

▶

◀

▶

Back

Close

Full Screen / Esc

Print Version

Interactive Discussion

Role of NO₃ radicals in oxidation processes

M. Vrekoussis et al.

Table 2. Observations of NO₃ radicals in the boundary layer

Site	Coordinates	NO ₃ Average (pptv)	NO ₃ Maximum (pptv)	Total path (km)	Year (summer)	Ref.
Continental Boundary Layer						
Lindenberg	52°13'N- 14°07'E	4.6	85	10	1998	Geyer et al., 2001
Marine Boundary Layer						
Tenerife	28°40'N- 16°05'W	8	20	9.6	1994	Carslaw et al., 1997
Kap Arkona (Rugen Island)	54°30'N- 13°30'E	6 - 10	98	7.3	1993/94	Heintz et al., 1996
Wayborne Clean conditions	52°57'N- 1°08'E	6	-	5	1995	Allan et al., 1999
Mace Head	53°19'N, 9°54'W	5	40	8.4	1996	Allan et al., 2000
Finokalia	35°30'N, 25°7'E	4.5	37	10.4	2001	This work

[Title Page](#)
[Abstract](#)
[Introduction](#)
[Conclusions](#)
[References](#)
[Tables](#)
[Figures](#)
[Back](#)
[Close](#)
[Full Screen / Esc](#)
[Print Version](#)
[Interactive Discussion](#)

Role of NO₃ radicals in oxidation processes

M. Vrekoussis et al.

Table 3. Rates for the reactions (3, k_3) and (-3, k_{-3}) and for the equilibrium reaction ($K_{3\text{eq}}$) at the minimum and maximum temperatures observed during MINOS and the corresponding NO₂ levels needed to reach equilibrium $K_{3\text{eq}}$. The reported lifetimes have been calculated on the basis of the geometric mean observed NO₂ mixing ratio of 0.4 ppbv

	T min (22.5 °C)	T max (30.2 °C)
k_3 (molecules ⁻¹ cm ³ s ⁻¹)	$1.39 \cdot 10^{-12}$	$2.02 \cdot 10^{-12}$
NO ₂ + NO ₃ → N ₂ O ₅		
k_{-3} (s ⁻¹)	$3.67 \cdot 10^{-2}$	$1.66 \cdot 10^{-1}$
N ₂ O ₅ → NO ₂ + NO ₃		
$K_{3\text{eq}}$ (= k_3/k_{-3})	$2.63 \cdot 10^{10}$	$8.21 \cdot 10^{10}$
NO ₂ for equilibrium (ppbv)	1.07	3.35
τ_{N2O5_k-3} (s)	27	6
τ_{NO3_k3} (s)	92	63

[Title Page](#)
[Abstract](#)
[Introduction](#)
[Conclusions](#)
[References](#)
[Tables](#)
[Figures](#)
[◀](#)
[▶](#)
[◀](#)
[▶](#)
[Back](#)
[Close](#)
[Full Screen / Esc](#)
[Print Version](#)
[Interactive Discussion](#)

Role of NO₃ radicals in oxidation processes

M. Vrekoussis et al.

Table 4. N₂O₅ lifetime with regard to the gas-phase reaction with water vapour for the extreme conditions observed during the MINOS campaign

Temperature °C	22.5	31.5
RN ₂ O ₅ H ₂ O (as pseudo 1 st order)	1.43 10 ⁻²¹	6.12 10 ⁻²¹
Relative Humidity	85	35
H ₂ O (molecules cm ⁻³)	5.67 10 ⁺¹⁷	3.85 10 ⁺¹⁷
RN ₂ O ₅ H ₂ O x [H ₂ O]	8.10 10 ⁻⁰⁴	2.36 10 ⁻⁰³
τN ₂ O ₅ (s)	1235	424

[Title Page](#)
[Abstract](#)
[Introduction](#)
[Conclusions](#)
[References](#)
[Tables](#)
[Figures](#)
[I◀](#)
[▶I](#)
[◀](#)
[▶](#)
[Back](#)
[Close](#)
[Full Screen / Esc](#)
[Print Version](#)
[Interactive Discussion](#)

Table 5. Gas phase reactions involved in the NO_3 radical budget. T is air temperature in Kelvin, AIR is air density in molecules cm^{-3} and $[\text{O}_2]$ is O_2 concentration in molecules cm^{-3} . The reaction rate of the OH-initiated DMS oxidation is also given for comparison purposes

Reaction	Rate	Rate at 298 K
NO_3 production		
$\text{NO}_2 + \text{O}_3 \rightarrow \text{NO}_3 + \text{O}_2$	$1.4 \cdot 10^{13} \exp(-2470/T)$	$3.55 \cdot 10^{17}$
NO_3 production from HNO_3 loss		
$\text{HNO}_3 + \text{OH} \rightarrow \text{NO}_3 + \text{H}_2\text{O}$	$R_1 = 2.4 \cdot 10^{17} \exp(460/T)$	$1.54 \cdot 10^{13}$
	$R_2 = 2.710^{17} \exp(2199/T)$	
	$R_3 = 6.5 \cdot 10^{13} \exp(1335/T) \text{ AIR}$	
	$R = R_1 + R_2 / (1 + R_2/R_1)$	
NO_3 production from N_2O_5 loss		
$\text{N}_2\text{O}_5 + \text{M} \rightarrow \text{NO}_2 + \text{NO}_3^b$	$R_1 = 10^3 (7/300)^{3.5} \exp(-11000/T) \text{ AIR}$	$5.02 \cdot 10^{25}$
	$R_2 = 9.7 \cdot 10^{11} (7/300)^{0.1} \exp(-11080/T)$ $F_c = 0.35$	
$\text{N}_2\text{O}_5 (hv) \rightarrow \text{NO}_2 + \text{NO}_3$		
NO_3 loss		
$\text{NO}_3 + \text{NO}_2 \rightarrow \text{N}_2\text{O}_5^b$	$R_1 = 3.6 \cdot 10^{30} (7/300)^{4.1} \text{ AIR}$	$1.41 \cdot 10^{12}$
	$R_2 = 1.9 \cdot 10^{12} (7/300)^{0.2}$ $F_c = 0.35$	
$\text{NO}_3 + \text{NO} \rightarrow 2 \text{NO}_2$	$1.8 \cdot 10^{11} \exp(110/T)$	$2.6 \cdot 10^{11}$
$\text{NO}_3 + \text{NO}_3 \rightarrow \text{NO}_2 + \text{NO}_2 + \text{O}_2$	$8.5 \cdot 10^{13} \exp(-2450/T)$	$2.3 \cdot 10^{16}$
$\text{NO}_3 (hv) \rightarrow \text{NO}_2 + \text{O}$		
$\text{NO}_3 (hv) \rightarrow \text{NO} + \text{O}_2$	$1.7 \cdot 10^{11}$	$1.7 \cdot 10^{11}$
$\text{NO}_3 + \text{O} \rightarrow \text{NO}_2 + \text{O}_2$	$1.4 \cdot 10^{14}$	$1.4 \cdot 10^{14}$
$\text{NO}_3 \rightarrow \text{NO} + \text{O}_2$		
reactions of NO_3 with RO_2 radicals		
$\text{NO}_3 + \text{HO}_2 \rightarrow \text{NO}_2 + \text{OH} + \text{O}_2$	$4 \cdot 10^{12}$	$4.0 \cdot 10^{12}$
$\text{NO}_3 + \text{RO}_2^c \rightarrow \text{NO}_2 + \text{HO}_2 + \text{product}$	$2.3 \cdot 10^{12}$	$2.3 \cdot 10^{12}$
Reactions of NO_3 with unsaturated VOC		
$\text{NO}_3 + \text{C}_2\text{H}_4 \rightarrow \text{NO}_2$ addition product	$3.3 \cdot 10^{12} \exp(-2880/T)$	$2.12 \cdot 10^{16}$
$\text{NO}_3 + \text{C}_3\text{H}_6 \rightarrow \text{NO}_2$ addition product	$4.6 \cdot 10^{13} \exp(-1155/T)$	$9.58 \cdot 10^{15}$
$\text{NO}_3 + \text{isoprene} \rightarrow$ addition product	$3.03 \cdot 10^{12} \exp(-446/T)$	$6.79 \cdot 10^{13}$
$\text{NO}_3 + \text{MVK} \rightarrow$ addition product	$4.7 \cdot 10^{16}$	$4.7 \cdot 10^{16}$
HNO_3 production from NO_3 loss		
Reactions of NO_3 with aldehydes		
$\text{NO}_3 + \text{HCHO} \rightarrow \text{HNO}_3 + \text{CO} + \text{HO}_2$	$5.8 \cdot 10^{16}$	$5.8 \cdot 10^{16}$
$\text{NO}_3 + \text{CH}_3\text{CHO} \rightarrow \text{HNO}_3 + \text{RO}_2$	$1.4 \cdot 10^{15} \exp(-1900/T)$	$2.4 \cdot 10^{15}$
$\text{NO}_3 + \text{MACR} \rightarrow \text{HNO}_3 + \text{product}$	$3.7 \cdot 10^{15}$	$3.7 \cdot 10^{15}$
Reactions of NO_3 with DMS		
$\text{NO}_3 + \text{DMS} \rightarrow \text{HNO}_3 + \text{radical}$	$1.9 \cdot 10^{12} \exp(500/T)$	$1.02 \cdot 10^{12}$
DMS reaction with OH radical (given here for comparison purposes)		
$\text{OH} + \text{DMS} \rightarrow$ addition products	$1.7 \cdot 10^{12} \exp(7810/T) [\text{O}_2] / (1 + 5.5 \cdot 10^{21} \exp(7460/T) [\text{O}_2])$	$1.8 \cdot 10^{12}$
$\text{OH} + \text{DMS} \rightarrow$ abstraction products	$1.13 \cdot 10^{11} \exp(-253/T)$	$4.8 \cdot 10^{12}$
N_2O_5 loss to HNO_3		
$\text{N}_2\text{O}_5 + \text{H}_2\text{O} \rightarrow 2 \text{HNO}_3$		
$\text{N}_2\text{O}_5 + \text{H}_2\text{O} + \text{H}_2\text{O} \rightarrow 2 \text{HNO}_3 + \text{H}_2\text{O}$	$3.6 \exp(-14570/T)^b$	$2.21 \cdot 10^{21}$
Other HNO_3 production		
$\text{NO}_2 + \text{OH} \rightarrow \text{HNO}_3^a$	$R_1 = 2.6 \cdot 10^{30} (7/300)^{2.9} \text{ AIR}$	$1.05 \cdot 10^{11}$
	$R_2 = 4.1 \cdot 10^{11}$	
	$F_c = 0.4$	
Other HNO_3 losses		
$\text{HNO}_3 (hv) \rightarrow \text{NO}_2 + \text{OH}$		

^a $K = R_1 / (1 + R_2/R_1)$, $F_c = A$, where $A = 1 / (1 + \log(R_1/R_2)^2)$

^b assumed as pseudo-first order with respect to H_2O concentration

^c $R = \text{CH}_3, \text{C}_2 \text{ to } \text{C}_6$; 18 different RO_2 radicals

Role of NO_3 radicals in oxidation processes

M. Vrekoussis et al.

Title Page

Abstract

Introduction

Conclusions

References

Tables

Figures

◀

▶

◀

▶

Back

Close

Full Screen / Esc

Print Version

Interactive Discussion

© EGU 2003

Role of NO₃ radicals in oxidation processes

M. Vrekoussis et al.

Table 6. Heterogeneous reactions taken into account in the model and the corresponding reactive accommodation coefficient (γ ; T : temperature in K). $K_{het} = \gamma (RT/2\pi M)^{0.5} A$, where M is the molecular mass of the compound, A the aerosol surface area and R the gas constant. γ values are taken from Atkinson et al. (2003) (IUPAC recommendations web version 2003)

	Reaction	γ
$K_{het}NO_3$	$NO_3(g) \rightarrow NO_3(part)$	0.006
$K_{het}2NO_3$	$NO_3(g) \rightarrow HNO_3(g)$	$2 \cdot 10^{-4}$
$K_{het}N_2O_5$	$N_2O_5(g) \rightarrow NO_3(part)$	0.1
$K_{het}HNO_3$	$HNO_3(g) \rightarrow NO_3(part)$	0.0014
$K_{het}HO_2$	$HO_2(g) \rightarrow loss$	$5.66 \cdot 10^{-5} \exp(1560/T)$

[Title Page](#)
[Abstract](#)
[Introduction](#)
[Conclusions](#)
[References](#)
[Tables](#)
[Figures](#)
[◀](#)
[▶](#)
[◀](#)
[▶](#)
[Back](#)
[Close](#)
[Full Screen / Esc](#)
[Print Version](#)
[Interactive Discussion](#)

© EGU 2003

**Role of NO₃ radicals
in oxidation
processes**

M. Vrekoussis et al.

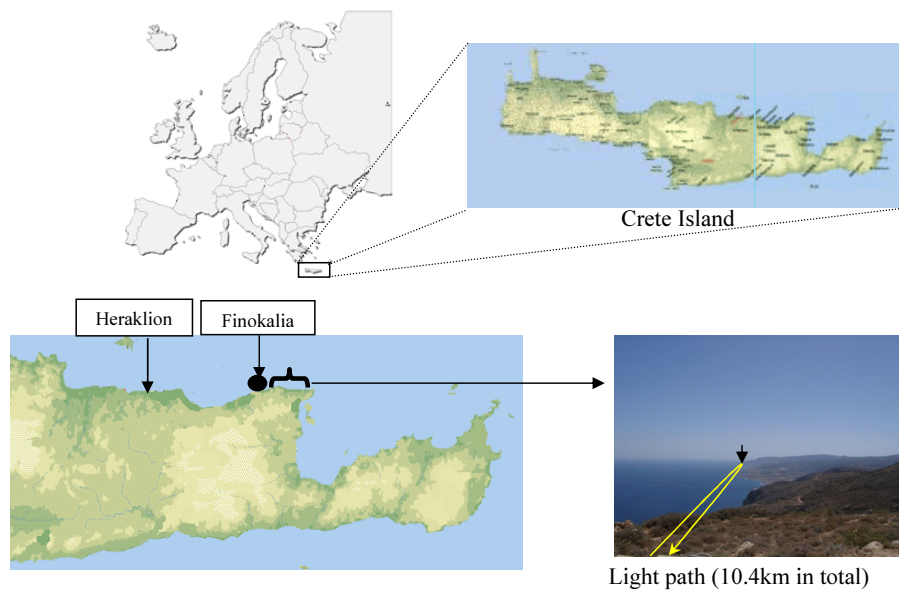


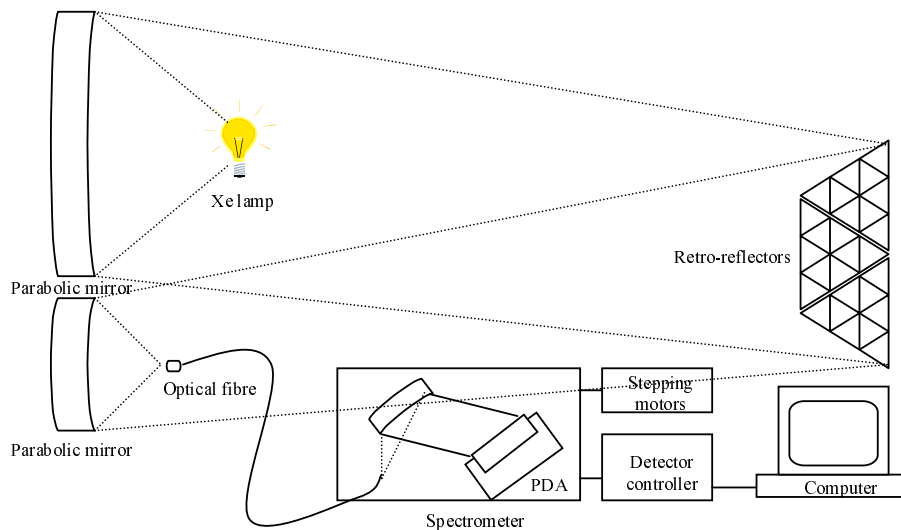
Fig. 1. Location of the Finokalia station, the retroreflectors and an indication of the light path of the DOAS instrument during the experiment.

[Title Page](#)[Abstract](#)[Introduction](#)[Conclusions](#)[References](#)[Tables](#)[Figures](#)[◀](#)[▶](#)[◀](#)[▶](#)[Back](#)[Close](#)[Full Screen / Esc](#)[Print Version](#)[Interactive Discussion](#)

© EGU 2003

**Role of NO_3 radicals
in oxidation
processes**

M. Vrekoussis et al.

**Fig. 2.** Sketch of the long path DOAS system.[Title Page](#)[Abstract](#)[Introduction](#)[Conclusions](#)[References](#)[Tables](#)[Figures](#)[◀](#)[▶](#)[◀](#)[▶](#)[Back](#)[Close](#)[Full Screen / Esc](#)[Print Version](#)[Interactive Discussion](#)

© EGU 2003

**Role of NO₃ radicals
in oxidation
processes**

M. Vrekoussis et al.

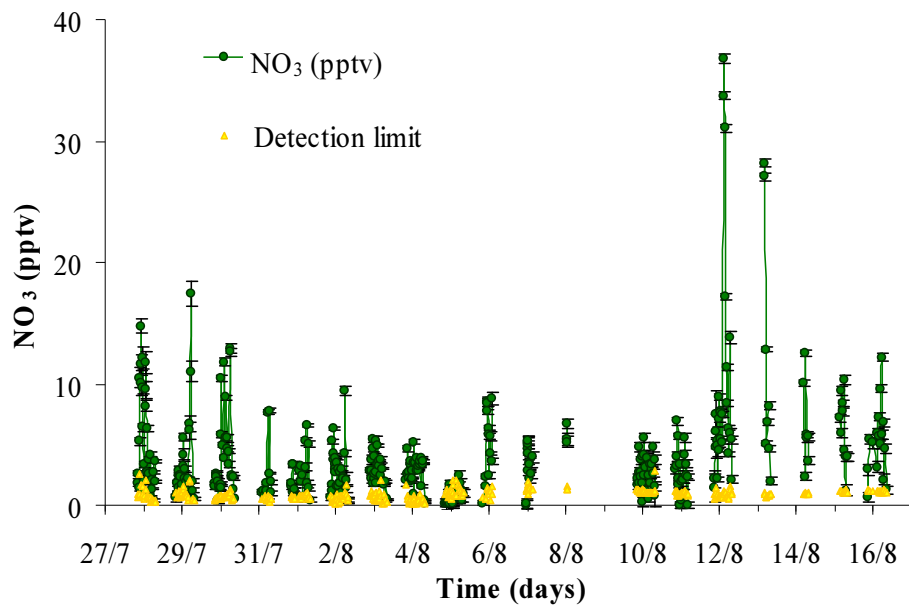


Fig. 3. NO₃ time series (in pptv) obtained at Finokalia during the MINOS campaign.

[Title Page](#)[Abstract](#)[Introduction](#)[Conclusions](#)[References](#)[Tables](#)[Figures](#)[◀](#)[▶](#)[◀](#)[▶](#)[Back](#)[Close](#)[Full Screen / Esc](#)[Print Version](#)[Interactive Discussion](#)

© EGU 2003

Role of NO_3 radicals in oxidation processes

M. Vrekoussis et al.

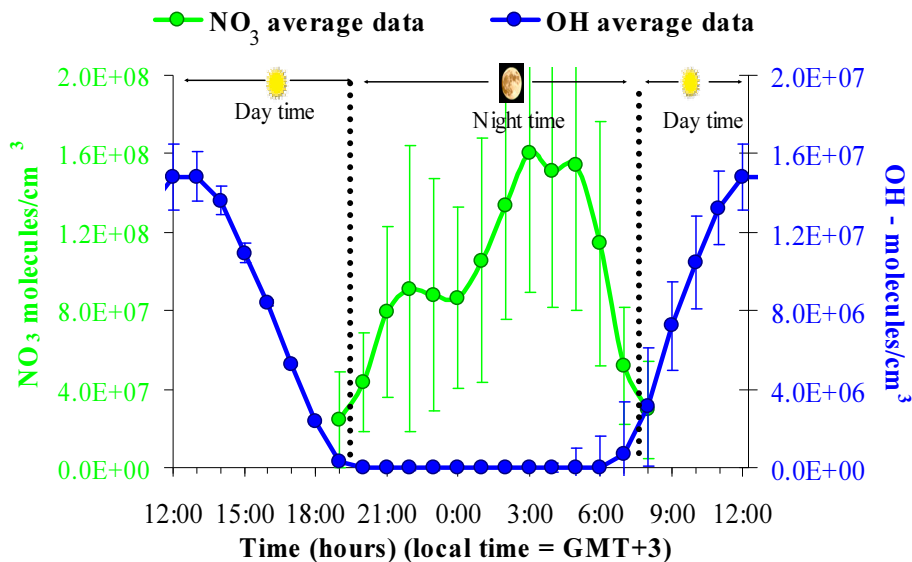


Fig. 4. Mean diurnal profile of NO_3 radical during the MINOS campaign. For comparison, OH radical simultaneous measured is also reported. Note the factor of 10 between the two scales.

[Title Page](#)[Abstract](#)[Introduction](#)[Conclusions](#)[References](#)[Tables](#)[Figures](#)[◀](#)[▶](#)[◀](#)[▶](#)[Back](#)[Close](#)[Full Screen / Esc](#)[Print Version](#)[Interactive Discussion](#)

© EGU 2003

**Role of NO₃ radicals
in oxidation
processes**

M. Vrekoussis et al.

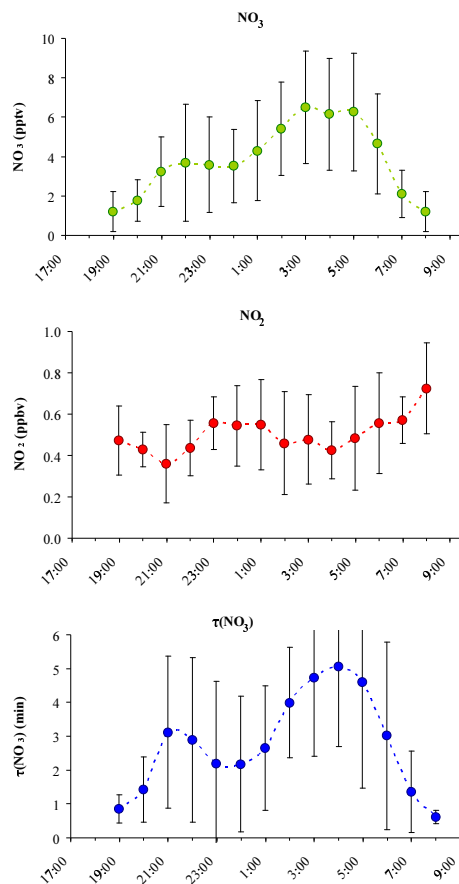


Fig. 5. Hourly mean observations and standard deviation **(a)** of NO₃ in pptv, **(b)** of NO₂ in ppbv and **(c)** lifetime of NO₃ radical in min – see text – during the MINOS campaign.

[Title Page](#)[Abstract](#)[Introduction](#)[Conclusions](#)[References](#)[Tables](#)[Figures](#)[◀](#)[▶](#)[◀](#)[▶](#)[Back](#)[Close](#)[Full Screen / Esc](#)[Print Version](#)[Interactive Discussion](#)

Role of NO₃ radicals
in oxidation
processes

M. Vrekoussis et al.

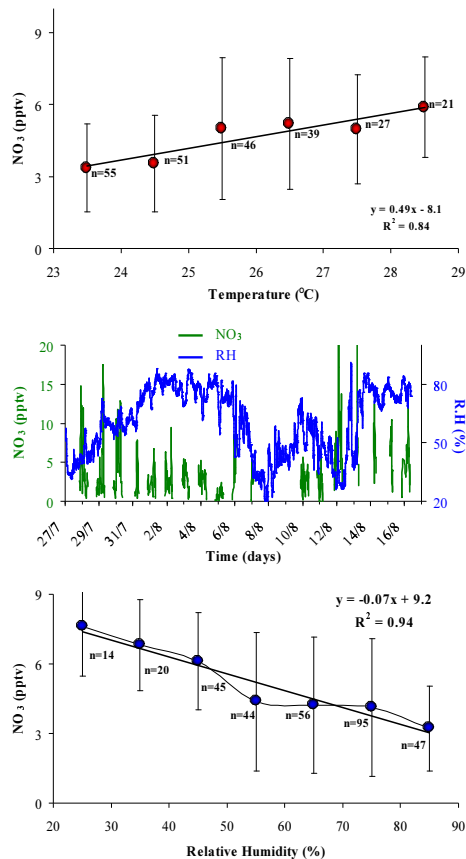


Fig. 6. (a) Correlation between NO₃ (in pptv) and air temperature (°C) NO₃ values are integrated every 10 units of temperature; (b) NO₃ observations as a function of Relative Humidity (RH in %) during the campaign and (c) correlation between NO₃ and RH NO₃ values are integrated every 10 units of RH.

[Title Page](#)[Abstract](#)[Introduction](#)[Conclusions](#)[References](#)[Tables](#)[Figures](#)[◀](#)[▶](#)[◀](#)[▶](#)[Back](#)[Close](#)[Full Screen / Esc](#)[Print Version](#)[Interactive Discussion](#)

© EGU 2003

**Role of NO₃ radicals
in oxidation
processes**

M. Vrekoussis et al.

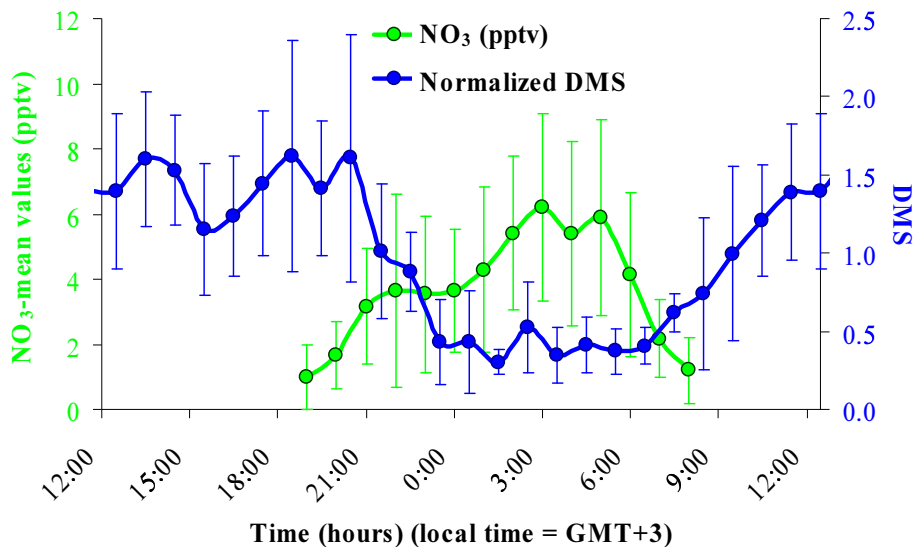


Fig. 7. Diurnal profile of NO₃ radical (in pptv) and normalized DMS concentrations averaged during the campaign.

[Title Page](#)[Abstract](#)[Introduction](#)[Conclusions](#)[References](#)[Tables](#)[Figures](#)[◀](#)[▶](#)[◀](#)[▶](#)[Back](#)[Close](#)[Full Screen / Esc](#)[Print Version](#)[Interactive Discussion](#)

© EGU 2003

**Role of NO₃ radicals
in oxidation
processes**

M. Vrekoussis et al.

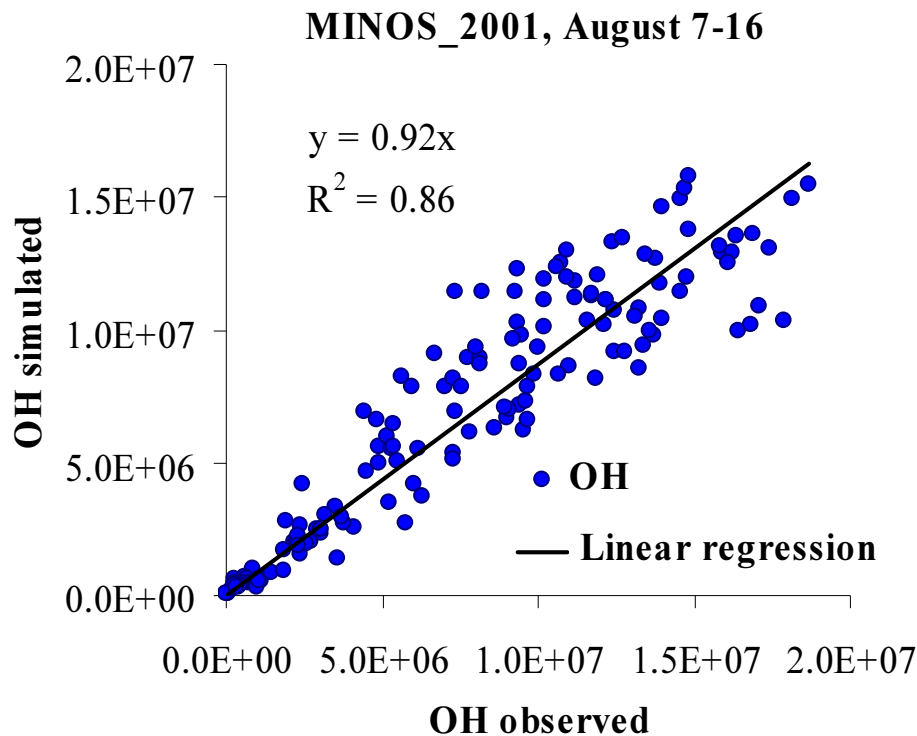


Fig. 8. Correlation between the modeled and measured OH concentrations during the campaign.

[Title Page](#)[Abstract](#)[Introduction](#)[Conclusions](#)[References](#)[Tables](#)[Figures](#)[◀](#)[▶](#)[◀](#)[▶](#)[Back](#)[Close](#)[Full Screen / Esc](#)[Print Version](#)[Interactive Discussion](#)

© EGU 2003

**Role of NO₃ radicals
in oxidation
processes**

M. Vrekoussis et al.

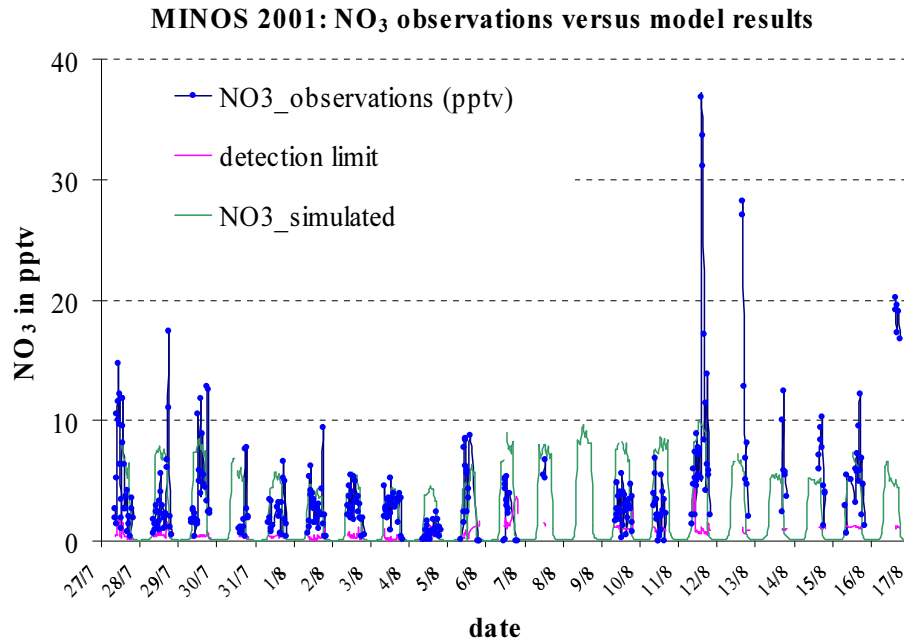


Fig. 9. Comparison between the modeled (green line) and measured NO₃ (closed circles) levels (in pptv) during the campaign.

[Title Page](#)[Abstract](#)[Introduction](#)[Conclusions](#)[References](#)[Tables](#)[Figures](#)[◀](#)[▶](#)[◀](#)[▶](#)[Back](#)[Close](#)[Full Screen / Esc](#)[Print Version](#)[Interactive Discussion](#)

© EGU 2003

Role of NO_3 radicals in oxidation processes

M. Vrekoussis et al.

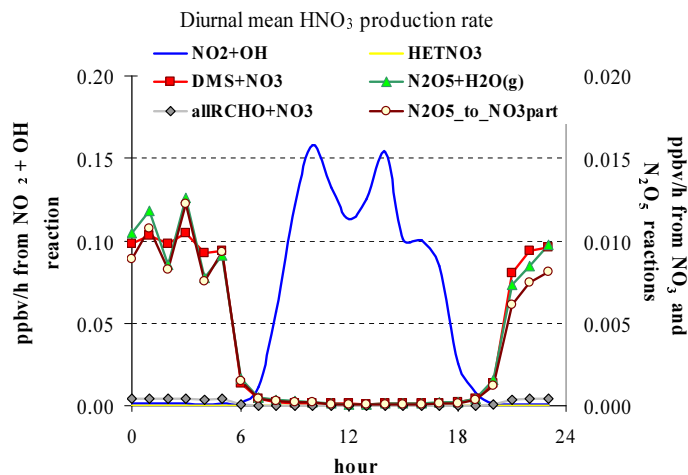
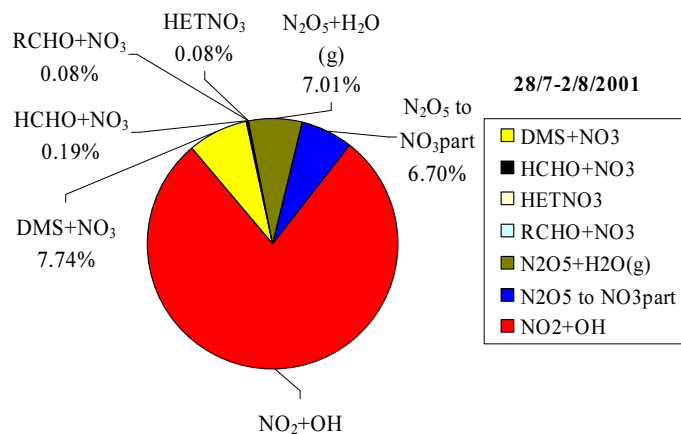


Fig. 10. (a) Distribution of HNO_3 (gaseous) formation; **(b)** diurnal mean HNO_3 production rate. Note the difference of a factor of 10 in the scale for the $\text{NO}_2 + \text{OH}$ reaction rate (axis to the left) compared to the other reactions (axis to the right).

[Title Page](#)
[Abstract](#)
[Introduction](#)
[Conclusions](#)
[References](#)
[Tables](#)
[Figures](#)
[◀](#)
[▶](#)
[◀](#)
[▶](#)
[Back](#)
[Close](#)
[Full Screen / Esc](#)
[Print Version](#)
[Interactive Discussion](#)